

Material-specific Conversion Factors for Different Solid Phantoms Used in the Dosimetry of Different Brachytherapy Sources

Sedigheh Sina¹, Fatemeh Lotfalizadeh², Mehrnoosh Karimipourfard², Neda Zaker², Bentolhoda Amanat³, Mehdi Zehtabian*², Ali. Soleimani Meigooni⁴

Abstract

Introduction

Based on Task Group No. 43 (TG-43U1) recommendations, water phantom is proposed as a reference phantom for the dosimetry of brachytherapy sources. The experimental determination of TG-43 parameters is usually performed in water-equivalent solid phantoms. The purpose of this study was to determine the conversion factors for equalizing solid phantoms to water.

Materials and Methods

TG-43 parameters of low- and high-energy brachytherapy sources (i.e., Pd-103, I-125 and Cs-137) were obtained in different phantoms, using Monte Carlo simulations. The brachytherapy sources were simulated at the center of different phantoms including water, solid water, poly(methyl methacrylate), polystyrene and polyethylene. Dosimetric parameters such as dose rate constant, radial dose function and anisotropy function of each source were compared in different phantoms. Then, conversion factors were obtained to make phantom parameters equivalent to those of water.

Results

Polynomial coefficients of conversion factors were obtained for all sources to quantitatively compare $g(r)$ values in different phantom materials and the radial dose function in water.

Conclusion

Polynomial coefficients of conversion factors were obtained for all sources to quantitatively compare $g(r)$ values in different phantom materials and the radial dose function in water.

Keywords: Brachytherapy, dosimetry, Phantom

1- Radiation Research Center, Shiraz University, Shiraz, Iran

2- Department of Ray-Medical Engineering, Shiraz University, Shiraz, Iran

*Corresponding author: Tel: +987112334033, Fax: +987116473035, E-mail: mehdizehtabian@yahoo.com

3- Department of Physics, Payame Noor University, Tehran, Iran

4- Comprehensive Cancer Center of Nevada, Nevada, USA

1. Introduction

According to the recommendations of Task Group No. 43 (TG-43) by the American Association of Physicists in Medicine (AAPM) (1, 2) and the full report by AAPM, European Society for Radiotherapy & Oncology (ESTRO) and High-Energy Brachytherapy Source Dosimetry (HEBD) working groups (3), the dosimetric parameters of brachytherapy sources should be determined in water phantoms.

The dosimetric parameters of new brachytherapy seeds need to be identified by Monte Carlo calculations or experimental measurements. However, performing measurements in liquid water is very difficult; consequently, the parameters are most often measured in water-equivalent phantoms, i.e., poly(methyl methacrylate) (PMMA), solid water and polystyrene. Several studies have been performed on dose distribution around low- and high-energy brachytherapy sources in different phantom materials, i.e., I-125 (4-6), Pd-103 (5), Ir-192 (7-10) and Cs-137 (11, 12). In 1988, Meigooni *et al.* proposed solid water phantoms for dose measurements around I-125 source. They showed that polystyrene and PMMA are not suitable materials for the dosimetry of this low-energy brachytherapy source. (4)

In 1994, Meigooni *et al.* compared linear attenuation coefficients and absorbed doses in plastic water and solid water phantom materials for a wide range of energy (20keV to cobalt-60 gamma rays). In the mentioned study, at low-photon energies (less than 100 keV), the total cross-section ratio of plastic water to liquid water was higher than unity (up to 2.5 times). However, in solid water phantoms, the ratios were much closer to unity (up to a 25% deviation). They suggested that dosimetric evaluations in new solid phantoms should be carefully performed before their clinical application. (13)

Moreover, Meigooni and colleagues in 2006 evaluated the ratios of dose rate constants and radial dose functions of solid water to liquid water for I-125 and Pd-103 brachytherapy

sources. They performed Monte Carlo N-Particle (MCNP) simulations with corrected cross-sectional data in solid water phantoms (i.e., $SW_{2.3}$ and $SW_{1.7}$) and proposed that the corrected $g(r)$ values may be applied in the extraction of consensual data in TG-43 protocol calculations (14).

Reniers *et al.* compared radial dose function $g(r)$ values of two low-energy brachytherapy sources (i.e., Pd-103 and I-125) in different solid phantoms, using EGS-nrc and MCNP4c Monte Carlo codes. They showed that $g(r)$ values in water, obtained by these codes, differed significantly due to variations in cross-sectional data. Therefore, they performed Monte Carlo simulations, using modified cross-section libraries and compared the calculated results with the experimental measurements, using thermoluminescence dosimetry (TLD). A good agreement between the calculations and TLD results was reported (5).

Moreover, Tedgren *et al.* obtained the dose distributions around Ir-192 brachytherapy sources in plastic phantoms with different sizes, using EGS-nrc Monte Carlo code. They showed that the water-equivalence of phantoms depends on the size and type of phantoms (10).

The aim of this study was to obtain the conversion factors for dosimetric parameters in different solid materials, which are usually applied as dosimetric phantoms (i.e., solid water, PMMA, polyethylene and polystyrene), using MCNP4c Monte Carlo code and the modified cross-section library.

2. Materials and Methods

In this study, Monte Carlo simulations of different high- and low-energy brachytherapy sources (Cs-137, Pd-103 and I-125) were performed in different phantoms.

2-1 Brachytherapy sources

In this study, three different brachytherapy sources (I-125 and Pd-103 as low-energy sources and Cs-137 as a high-energy source) were simulated.

2-1-1. I-125 source

I-25 source by IsoAid Advantage™ (model IAI-125A) is a brachytherapy source with the overall length of 4.50 mm and the active length of 3.00 mm, which is coated by a titanium capsule (0.05 mm) (15-17). The two end welds are two hemispheres and a spherical silver marker (0.5 mm in diameter and 3mm in length), coated with a 1µm layer of AgI, containing I-125, is located at the center of the source (see Figure 1a).

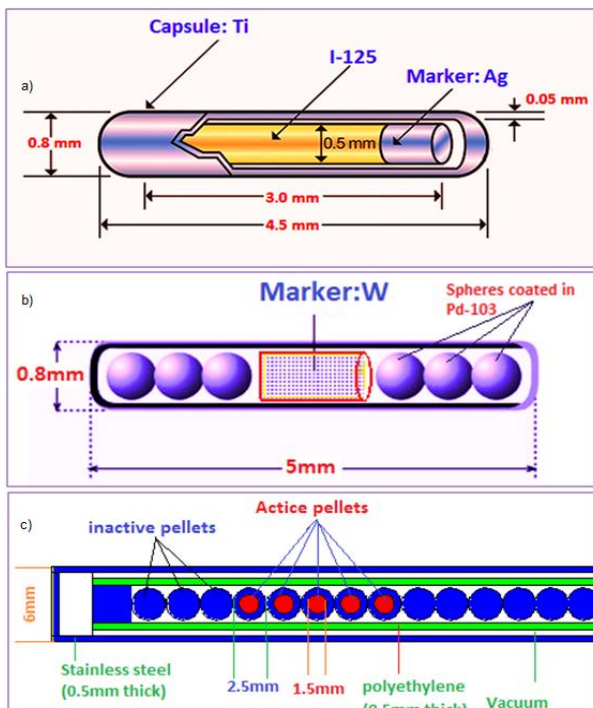


Figure 1. a) I-125 source by IsoAid Advantage, Model IAI-125A; b) Pd-103 source by Best Industries, Model Best 2335; c) the combination of five Cs-137 active pellets inside the vaginal cylindrical applicator

2-1-2. Pd-103 source

The Pd-103 source (Model Best2335, Best Industries) with the overall source length of 5.00 mm and the active length of 4.76 mm is encapsulated in a titanium cover with the total thickness of 0.080 mm and the outer diameter of 0.800 mm (18, 19). A cylindrical tungsten X-ray marker (0.5 mm in diameter and 1.2 mm in length) is located at the center of the source. On either side of the tungsten marker, there are three polymeric spheres (0.5 mm in diameter), coated with Pd-103. The geometry of the source is shown in Figure 1b.

2-1-3. Nucletron Cs-137 pellet sources

A combination of five active Cs-137 pellet sources of Selectron remote was simulated inside a vaginal cylindrical applicator after loading the system with non-active (dummy) pellets. This combination acted as a Cs-137 line source with an active length of 10 mm (see Figure 1c) (11, 12, 20). Each spherical source has an active ceramic core (1.5 mm in diameter) with a 0.5 mm steel cover. The dummy pellets are stainless steel spheres (2.5 mm in diameter). The cylindrical applicator, as shown in Figure 1c, consists of cylindrical shells of polyethylene, vacuum and stainless steel.

2-2- Monte Carlo simulations

In this study, Monte Carlo simulations were performed, using MCNP4c code and a modified cross-section library, since the one used for MCNP4C code is not reliable in low-energy photons. This code considers photon interactions, i.e., photoelectric absorption, coherent/incoherent scattering and pair production (21). It should be mentioned that the cross-section library of the code was changed to ENDF/B-VI.8.

2-2-1- The water equivalence of phantoms

$$\text{and } \left(\frac{\mu_{en}}{\rho} \right)_{phantom}^{water}$$

In the first step, the point sources of I-125, Pd-103 and Cs-137 were simulated at the center of homogeneous spherical phantoms (100 cm in diameter). These phantoms including solid water, lucite (PMMA), polyethylene and polystyrene were divided into thin spherical shells (1 mm thickness) as tally cells to measure $D_{phantom,phantom}(r)$.

The dose at each point was obtained by dividing the result of tally type *F8 by the mass of the tally cell, located at that point. To obtain the values of $D_{w,w}(r)$, the whole phantom and the shells were water, while the values of $D_{w,phantom}(r)$ were obtained by defining a small water shell at r(cm) distance inside the solid phantom. The material composition and the density of all phantoms and source components are shown in Table 1.

Table 1. Material compositions used in the present study

| Phantoms | | | |
|---|------------------------------|--|-----------|
| Phantom | Density (g/cm ³) | Composition | Reference |
| Water | 0.998207 | H(0.111894%), O(0.888106) | (24) |
| Soft tissue | 1 | H(10.4472%), C(23.219%), N(2.488%), O(63.0238%), Na(0.113%), Mg(0.013%), P(0.133%), S(0.199%), Cl(0.134%), K(0.199%), Ca(0.023%), Fe(0.005%), Zn(0.003%) | (24) |
| Muscle | 1.11 | H(9.8234%), C(15.6214%), N(3.5451%), O(71.0101%) | (24) |
| Lucite (Plexiglas or PMMA) | 1.19 | H(0.080538%), C(0.599848%), O(0.319614%) | (24) |
| Solid water | 1.015 | C(67.2%), O(19.9%), H(8.1%), N(2.4%), Ca(2.3%), Cl(0.1%) | (5) |
| Polyethylene | 0.93 | H(0.143716%), O(0.856284%) | (24) |
| Polystyrene | 1.06 | H(0.077421%), O(0.922579%) | (24) |
| Components of the sources | | | |
| Air | 0.001205 | C(0.0124%), N(75.5268%); O(23.1781%); Ar(1.2827%) | (24) |
| Stainless steel | 7.8 | C(0.026%), Mn(1.4%), Si(0.42%), P(0.019%), S(0.003%), Cr(16.8%), Mo(2.11%), Ni(11.01%), Fe(68.21%) | (3) |
| PVC | 1.4 | Cl(56.72%), C(38.44%), H(4.84%) | (3) |
| Ceramic (The central core of Cs-137 pellets) | 2.9 | Si(26.18%), Ti(3.00%), Al(1.59%), B(3.73%), Mg(1.21%), Ca(2.86%), Na(12.61%), Cs(0.94%), O(47.89%) | (3) |
| Silver | 10.49 | Ag(100%) | ----- |
| Titanium | 4.507 | Ti(100%) | ----- |
| Tungesten | 19.25 | W(100%) | ----- |
| Polymer in Pd-103 source | 1.00 | C (89.73%), H (7.85%), O (1.68%), N (0.740%) | (18) |

Also, 10^9 particle histories and an energy cut-off of 5 keV were considered for all simulations in this study.

It should be mentioned that $D_{w,phantom}(r)$ is the dose delivered to the small mass of water in each solid phantom at r (cm) distance from the source center. Also, $D_{w,w}(r)$ is the dose received by the small mass of water in the water phantom, and $D_{phantom,phantom}(r)$ is the dose received by the small mass of phantom in the phantom. These values were used to investigate the water equivalence and $\left(\frac{\mu_{en}}{\rho}\right)_{phantom}^{water}$ of each point source at different distances (i.e., 0.5, 1, 3, 5, 7 and 10 cm).

The water equivalence of each solid phantom for each brachytherapy source was obtained, using the following formula (22):

$$Water\ equivalence(r) = \frac{D_{w,phantom}(r)}{D_{w,w}(r)} \quad (1)$$

As previously mentioned, the dose rate distribution around real brachytherapy sources was obtained in homogeneous phantoms. Also, ($D_{phantom,phantom}$), needed to be converted to

$D_{w,phantom}$, using appropriate conversion factors (see equation 2) [22]:

$$Conversion\ factor = \left(\frac{\mu_{en}}{\rho}\right)_{phantom}^{water}(r) = \frac{D_{w,phantom}(r)}{D_{phantom,phantom}(r)}$$

where $\left(\frac{\mu_{en}}{\rho}\right)_{phantom}^{water}(r)$ is the ratio of energy fluence weighted mean of mass energy-absorption coefficients for water and phantom at distance r . This ratio is used as conversion factors for converting $D_{phantom,phantom}$ to $D_{w,phantom}$. The values of $\left(\frac{\mu_{en}}{\rho}\right)_{phantom}^{water}$ were obtained at 0.5, 1, 3, 5, 7 and 10 cm distances from I-125, Pd-103 and Cs-137 sources.

2-2-2- TG-43 parameters of the sources

In the second step, the mentioned linear brachytherapy sources were simulated inside spherical phantoms (60 cm in diameter). Each source was simulated at the center of water phantom, and small spherical water tally cells

were placed at different distances and angles from the source center (see Figure 2).

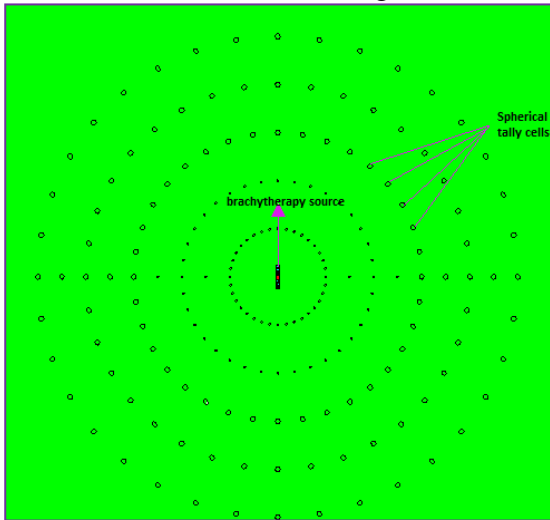


Figure 2. The simulation geometry used in this study for Monte Carlo simulations

All the simulations were repeated for other phantom materials, i.e., solid water, lucite PMMA, polyethylene and polystyrene to obtain $D_{phantom,phantom}$ in tally cells. The dose rates received by water in each phantom ($D_{w,phantom}(r)$) were then obtained by the values of $D_{phantom,phantom}(r)$, using appropriate conversion factors (see equation 2) to be consistent with experimental dosimetric evaluations.

$D_{w,phantom}(r)$ was used for the calculation of TG43U1 dosimetric parameters of Pd-103, I-125 and Cs-137 sources in solid phantoms. The air-kerma strength (S_K) was also obtained according to TG-43U1 recommendations.

2-2-3- Phantom-to-water conversion factors

2-2-3-1- Conversion factor for dose rate constant (Λ)

The Monte Carlo simulated dose at the reference point $D_{phantom,phantom}(1cm, \frac{\pi}{2})$, around three linear brachytherapy sources was converted to $D_{w,phantom}(1cm, \frac{\pi}{2})$, using the conversion factor $(\frac{\mu_{en}}{\rho})_{phantom}^{water}$, obtained in the previous section by equation 2. The division of dose rate at the reference point $D_{w,phantom}(1cm, \frac{\pi}{2})$ of each phantom by S_K gave rise to dose rate constant ($\Lambda_{w,phantom}$).

The measured dose-to-water values in any solid phantom ($D_{w,phantom}$) should be converted to dose-to-water values in water phantoms ($D_{w,w}$) before being applied in treatment planning systems. Therefore, conversion factors should be utilized for the dosimetric parameters of brachytherapy sources. The conversion factor ($CF_{\Lambda_{w,phantom}^{w,w}}$) for converting the dose rate constant of each brachytherapy source in phantom $\Lambda_{w,phantom}$ to that of water $\Lambda_{w,w}$ was obtained by equations 3 and 4:

$$(3) \Lambda_{w,w} = \Lambda_{w,phantom} \times (CF_{\Lambda_{w,phantom}^{w,w}})$$

$$(4) CF_{\Lambda_{w,phantom}^{w,w}} \text{ or } \Lambda_{w,phantom}^{w,w} =$$

$$\frac{\Lambda_{w,w}}{\Lambda_{w,phantom}} =$$

2-2-3-2- Conversion factors for radial dose function ($g(r)$)

The consensual data for radial dose functions in TG-43 report are usually extracted from Monte Carlo simulations. However, by suggesting appropriate correction factors, the measured data can be effectively used in deriving consistent $g(r)$ values. The distance-based conversion factor ($CF_{g(r)_{w,phantom}^{w,w}}$) for converting the radial dose function of each phantom to that of a water phantom was obtained by equations 5 and 6:

$$g(r)_{w,w} = g(r)_{w,phantom} \times (CF_{g(r)_{w,phantom}^{w,w}})$$

(5)

$$CF_{g(r)_{w,phantom}^{w,w}} = \frac{g_{w,w}(r)}{g_{w,phantom}(r)} = g_{w,phantom}^{w,w}(r)$$

(6)

2-2-4- Water-to-tissue conversion factor

In this step, Dose to soft tissue in soft tissue ($D_{st,st}$) and Dose to muscle in muscle ($D_{m,m}$) were obtained for point sources in spherical phantoms, as described in section 2-2-1. Then, the conversion factors for obtaining the dose in each tissue from the dose in water were calculated by dividing $D_{tissue,tissue}$ and $D_{w,w}$. By using the conversion factors, the calculated dose in TG-43 formalism can be easily

converted to tissue dose for the purpose of consistency with TG-186 recommendations.

3. Results

3-1- Water equivalence of phantoms and

$$\left(\frac{\mu_{en}}{\rho}\right)_{phantom}^{water}(r)$$

Table 2 compares the water equivalence of each phantom obtained by equation 1, using Monte Carlo simulations of point sources. As demonstrated in this table, the values of water-equivalent solid phantoms were much higher than the values obtained in low-energy

brachytherapy sources. Therefore, large conversion factors are necessary for TG-43 parameters to convert the dose-to-water value in a phantom to a dose-to-water value in a water phantom.

The values of $\left(\frac{\mu_{en}}{\rho}\right)_{phantom}^{water}(r)$, i.e., conversion factors for converting $D_{phantom,phantom}(r)$ to $D_{w,phantom}(r)$, are shown in Table 3 for I-125, Pd-103 and Cs-137 sources.

Table 2. Comparison of the water equivalence $\left(\frac{D_{w,phantom}(r)}{D_{phantom}(r)}\right)$ of three sources at different distances

| r(cm) | Pd-103 | | | | I-125 | | | | Cs-137 | | | |
|-------|-------------|-------|--------------|-------------|-------------|-------|--------------|-------------|-------------|-------|--------------|-------------|
| | Polystyrene | PMMA | Polyethylene | Solid water | Polystyrene | PMM A | Polyethylene | Solid water | Polystyrene | PMMA | Polyethylene | Solid water |
| 0.5 | 1.213 | 1.104 | 1.235 | 0.968 | 1.090 | 1.056 | 1.094 | 0.978 | 1.005 | 0.997 | 1.007 | 1.001 |
| 1.0 | 1.476 | 1.207 | 1.540 | 0.939 | 1.212 | 1.122 | 1.228 | 0.969 | 1.015 | 1.012 | 1.009 | 1.019 |
| 3.0 | 3.398 | 1.784 | 3.945 | 0.889 | 1.775 | 1.301 | 1.877 | 0.892 | 1.045 | 0.999 | 0.995 | 0.98 |
| 5.0 | 6.307 | 2.151 | 8.210 | 0.754 | 2.496 | 1.477 | 2.825 | 0.832 | 1.020 | 0.995 | 1.033 | 1.007 |
| 7.0 | 11.533 | 2.696 | 17.030 | 0.663 | 3.464 | 1.654 | 4.122 | 0.771 | 0.994 | 0.959 | 1.001 | 0.993 |
| 10. | | | | | | | | | | | | |
| 0 | 24.462 | 3.304 | 41.938 | 0.584 | 5.338 | 1.857 | 6.910 | 0.707 | 1.017 | 0.988 | 1.034 | 1.008 |

3-2- Comparison of TG-43 parameters in different phantoms

3-2-1. Dose rate constant (Λ)

The dose rate constant values for brachytherapy sources in different phantoms ($\Lambda_{w,phantom}$) are shown in Table 4.

3-2-2. Radial dose function ($g(r)$)

As shown in Table 2, the water equivalence of phantoms was distance-dependent. Therefore, it is necessary to use distance-based conversion factors for radial dose function. Figures 3a and 3b compare the radial dose function for Pd-103 and I-125 as low-energy brachytherapy sources, respectively. The results were compared with those presented in TG43U1-S1 report. Moreover, the $g(r)$ values for high-energy Cs-137 source are shown in Figure 4. The sixth-order polynomials were fitted to $g(r)$ values of water for the three sources (see Figures 3a, 3b and 4).

3-2-3. Anisotropy function ($F(r,\theta)$)

Figure 5 compares the anisotropy function of low-energy brachytherapy sources (I-125 and Pd-103) for different phantoms. The $F(r,\theta)$ values for Cs-137 source in different phantoms are compared in Figure 6. The values of sixth-order polynomials fitted the $F(r,\theta)$ values of water and the error bars for each point in water are shown in the figures.

Conversion Factors for using Solid Phantoms in Brachytherapy

Table 3. The values of $\left(\frac{\mu_{en}}{\rho}\right)_{phantom}^{water}$ obtained to be used as conversion factors for converting $D_{phantom,phantom}$ to $D_{w,phantom}$ at different distances from point sources in different phantoms

| r(cm) | <u>Pd-103</u> | | | | | <u>I-125</u> | | | | | <u>Cs-137</u> | | | | | |
|-----------|-------------------|-------------------|------------------|-------------------|-------------------|------------------|-------------------|-------------------|------------------|-------------------|-------------------|------------------|-------------------|-------------------|-------------------|-------------------|
| | Polystyrene | PMM A | PMM A | Polyethylene | Solid water | Polystyrene | PMM A | PMM A | Polyethylene | Solid water | Solid water | Polystyrene | PMM A | Polyethylene | Solid water | |
| 0.5 | 2.593 | 1.634 | ----- -- | 2.773 | 0.949 | ----- -- | 2.520 | 1.616 | ----- -- | 2.671 | 0.912 | ----- -- | 0.943 | 0.840 | 1.075 | 0.948 |
| 1.0 | 2.580 | 1.610 | ----- -- | 2.771 | 0.949 | ----- -- | 2.499 | 1.610 | ----- -- | 2.666 | 0.915 | ----- -- | 0.943 | 0.840 | 1.075 | 0.945 |
| 3.0 | 2.537 | 1.619 | ----- -- | 2.704 | 0.949 | ----- -- | 2.510 | 1.616 | ----- -- | 2.623 | 0.922 | ----- -- | 0.943 | 0.840 | 1.075 | 0.971 |
| 5.0 | 2.536 | 1.636 | ----- -- | 2.816 | 0.956 | ----- -- | 2.487 | 1.605 | ----- -- | 2.637 | 0.915 | ----- -- | 0.943 | 0.840 | 1.075 | 0.941 |
| 7.0 | 2.496 | 1.610 | ----- -- | 2.678 | 0.974 | ----- -- | 2.505 | 1.594 | ----- -- | 2.666 | 0.926 | ----- -- | 0.943 | 0.840 | 1.075 | 0.920 |
| 10.0 | 2.473 | 1.568 | ----- -- | 2.610 | 0.970 | ----- -- | 2.494 | 1.606 | ----- -- | 2.634 | 0.926 | ----- -- | 0.943 | 0.840 | 1.075 | 0.933 |
| Average | 2.536 | 1.613 | 1.629 | 2.725 | 0.958 | 0.940 | 2.503 | 1.608 | 1.607 | 2.649 | 0.919 | 0.917 | 0.943 | 0.840 | 1.075 | 0.943 |
| Reference | The present study | The present study | Luxton 1994 (25) | The present study | The present study | Luxton 1994 (25) | The present study | The present study | Luxton 1994 (25) | The present study | The present study | Luxton 1994 (25) | The present study | The present study | The present study | The present study |

Table 4. Dose rate constants of phantoms ($\Lambda_{w,Phantom}$)

| | Method | Pd-103 | I-125 | Cs-137 | References |
|----------------------------|------------------------|---------|---------|-----------|-------------------|
| $\Lambda_{w,w}$ | Monte Carlo simulation | 0.67±5% | 0.96±3% | 1.034*±5% | The present study |
| | Monte Carlo simulation | 0.67±3% | ----- | ----- | (18) |
| | Monte Carlo simulation | ----- | 0.98±3% | ----- | (15) |
| | Monte Carlo simulation | ----- | ----- | 1.095±5% | (12) |
| $\Lambda_{w,PMMA}$ | Monte Carlo simulation | 0.81±5% | 1.08±5% | 1.034±5% | The present study |
| | Monte Carlo simulation | ----- | ----- | 1.094±5% | (12) |
| $\Lambda_{w,Solid\ water}$ | Monte Carlo simulation | 0.63±5% | 0.93±5% | 1.034±5% | The present study |
| | Monte Carlo simulation | 0.65±8% | ----- | ----- | (18) |
| | TLD dosimetry | 0.67±8% | ----- | ----- | (18) |
| | Monte Carlo simulation | ----- | 0.95±3% | ----- | (15) |
| | TLD dosimetry | ----- | 0.99±8% | ----- | (15) |
| $\Lambda_{w,Polyethylene}$ | Monte Carlo simulation | 1.04±5% | 1.18±5% | 1.034±5% | The present study |
| $\Lambda_{w,Polystyrene}$ | Monte Carlo simulation | 0.99±5% | 1.16±5% | 1.034±5% | The present study |

* A combination of five active pellets

** A single active pellet

Table 5. The conversion factor for $CF_{\Lambda_{w,w,phantom}}^{w,w}$

| | Pd-103 | I-125 | Cs-137 | References |
|---------------------------------------|--------|-------|------------|--------------------------|
| $CF_{\Lambda_{w,PMMA}}^{w,w}$ | 0.829 | 0.891 | Not needed | The present study |
| | ----- | 0.893 | ----- | Luxton et al. 1990(26) |
| $CF_{\Lambda_{w,Solid\ water}}^{w,w}$ | 1.065 | 1.032 | Not needed | The present study |
| | 1.05 | 1.032 | ----- | Meigooni et al. 2006(14) |
| | 1.066 | ----- | ----- | Meigooni et al. 2001(18) |
| $CF_{\Lambda_{w,Polyethylene}}^{w,w}$ | 0.649 | 0.814 | Not needed | The present study |
| $CF_{\Lambda_{w,Polystyrene}}^{w,w}$ | 0.678 | 0.825 | Not needed | The present study |

Table 6. The conversion factor for $CF_{g(r)phantom}^{water}$

| $CF_{g(r)phantom}^{water}$ | | Pd-103 | I-125 | Cs-137 |
|-------------------------------|------------------------|---|---|------------|
| $g_{solidwater}^{water}(r)$ | <u>Fitted equation</u> | $a_0 + a_1r$ | $a_0 + a_1r$ | |
| | Coefficients | $a_0 = 0.95$ $a_1 = 0.045$ | $a_0 = 0.965$ $a_1 = 0.027$ | Not needed |
| $g_{PMMA}^{water}(r)$ | <u>Fitted equation</u> | $a_0 + a_1r + a_2r^2$ | $a_0 + a_1r + a_2r^2$ | |
| | Coefficients | $a_0 = 1.158$ $a_1 = -0.149$ $a_2 = 0.007$ | $a_0 = 1.097$ $a_1 = -0.087$ $a_2 = 0.003$ | Not needed |
| $g_{Polystyrene}^{water}(r)$ | <u>Fitted equation</u> | $a_0 + a_1r + a_2r^2 + a_3r^3 + a_4r^4$ | $a_0 + a_1r + a_2r^2 + a_3r^3 + a_4r^4$ | |
| | Coefficients | $a_0 = 1.471, a_1 = -0.5427$ $a_2 = 0.0918, a_3 = -0.0077$ $a_4 = 0.0003$ | $a_0 = 1.245, a_1 = -0.2879$ $a_2 = 0.0399, a_3 = -0.0032$ $a_4 = 0.0001$ | Not needed |
| $g_{Polyethelene}^{water}(r)$ | <u>Fitted equation</u> | $a_0 + a_1r + a_2r^2 + a_3r^3 + a_4r^4$ | $a_0 + a_1r + a_2r^2 + a_3r^3 + a_4r^4$ | |
| | Coefficients | $a_0 = 1.530, a_1 = -0.6206$ $a_2 = 0.110, a_3 = -0.0094$ $a_4 = 0.0003$ | $a_0 = 1.263, a_1 = -0.303$ $a_2 = 0.036, a_3 = -0.002$ $a_4 = 0.00006$ | Not needed |

Conversion Factors for using Solid Phantoms in Brachytherapy

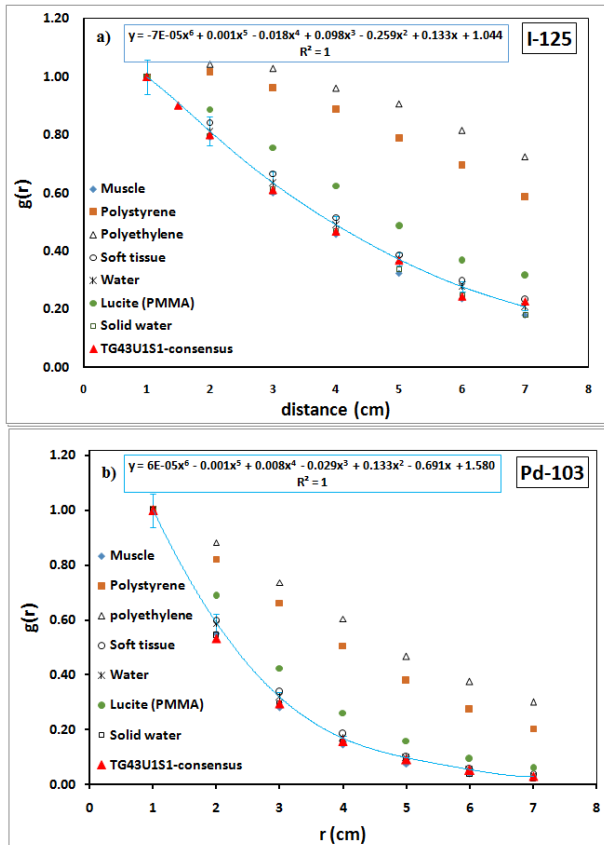


Figure 3. The values of radial dose function $g(r)$ for different phantoms using different sources: a) Pd-103 and b) I-125

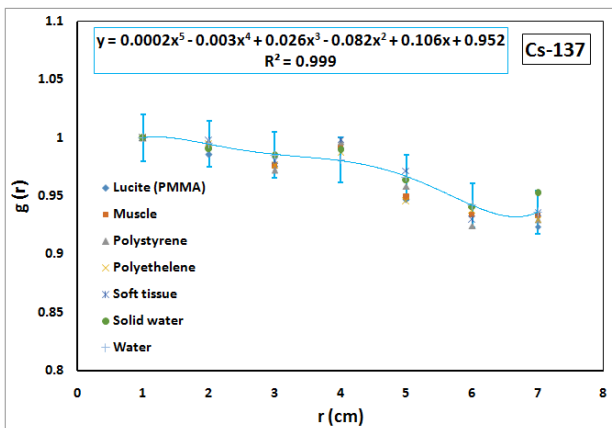


Figure 4. The values of radial dose function $g(r)$ in different phantoms for Cs-137 source

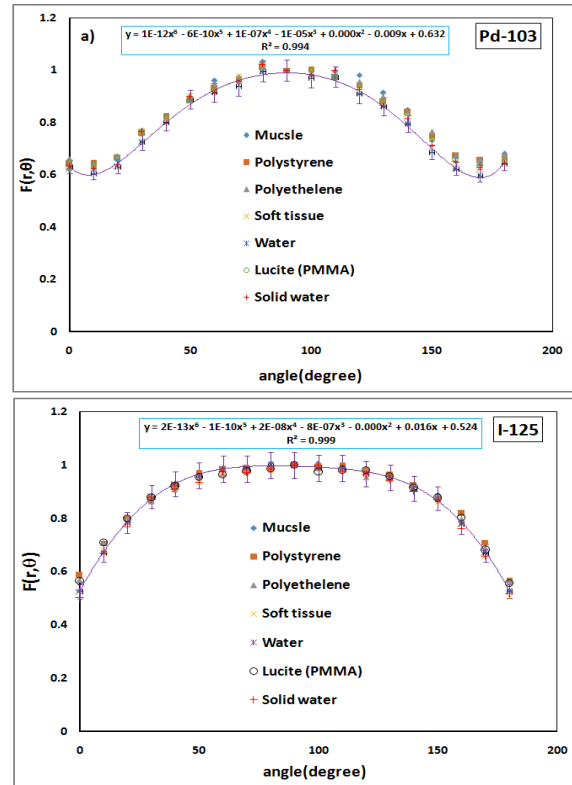


Figure 5. Comparison of $F(r, \theta)$ in different phantoms for different sources: a) Pd-103 and b) I-125

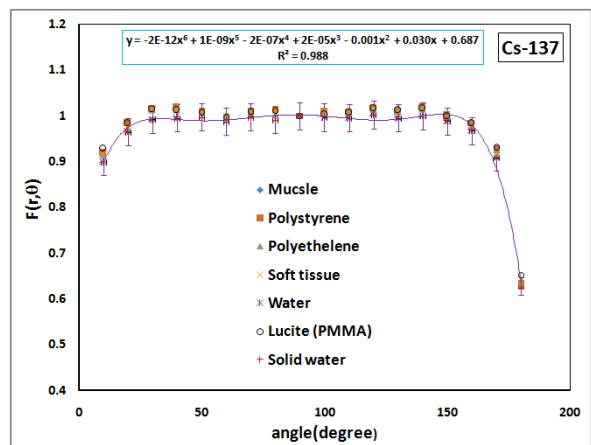


Figure 6. Comparison of $F(r, \theta)$ for Cs-137 in different phantoms

3-3- Phantom-to-water conversion factors

3-3-1- Conversion factors for (Λ)

The conversion factors obtained for different phantoms ($CF_{\Lambda_{w,phantom}^{w,w}}$) are shown in Table 5.

3-3-2- Conversion factors for $g(r)$

The distance-based conversion factors for the radial dose functions obtained by equations 5 and 6 are shown in Table 6 for brachytherapy sources.

3-4- Water-to-tissue conversion factors

The ratios of $D_{tissue,tissue}$ to $D_{water,water}$ for different sources and different distances for muscle and soft tissues are shown in Figure 7. These correction factors can be used for converting the dose to water in water phantom to the tissue dose.

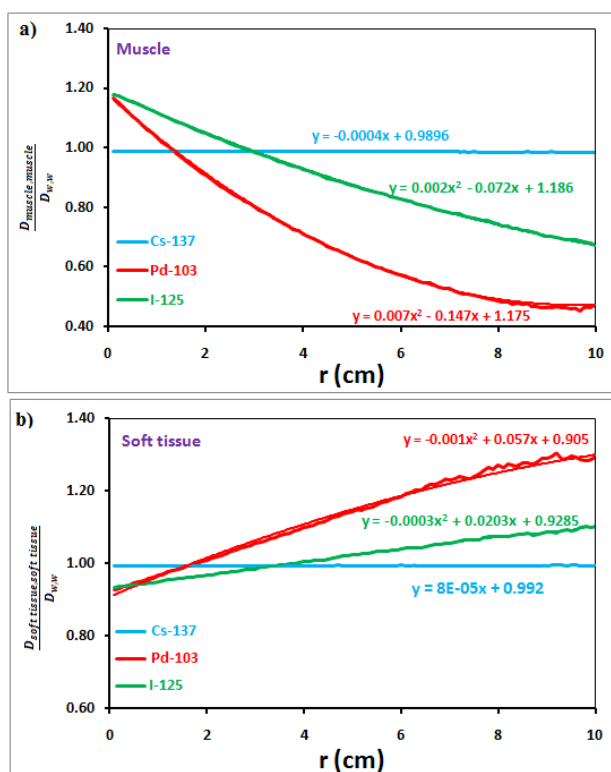


Figure 7. The conversion factor for obtaining the dose to soft tissue and muscle from the dose to water

4. Discussion

According to the figures 3, and 4, in low-energy sources, the radial dose function values in solid water were closer to those of water, compared to other phantoms. Lucite, polystyrene and polyethylene were not suitable dosimetric phantoms for Pd-103 and I-125 unless conversion factors were applied for their conversion to water equivalents. Although the density of lucite was higher than that of water, the $g(r)$ value of lucite was closer to that of water in comparison with polyethylene and polystyrene. These results were in close agreement with the findings reported by Meigooni and colleagues (4).

Figures 5, and 6 indicate that the differences in $F(r,\theta)$ values for all sources in all phantoms were negligible. Therefore, no conversion factor was required for this parameter.

According to the results shown in Tables 4, and 5, the results obtained in this study were in close agreement with those reported in previous studies (12, 15, 18, 23). However, the discrepancy in dose rate constant values for Cs-137 between previous studies and the current research is due to the fact that previous investigations were performed on a single active pellet, while the present study was conducted, using five active sources.

According to the results of Table 5, for high-energy brachytherapy sources (Cs-137), the values obtained for dose rate constant conversion factors were close to one. However, for low-energy sources, lucite, polyethylene and polystyrene required greater conversion factors. These values were compared with those proposed by Meigooni et al. for Pd-103 and I-125 sources (14). Table 5 shows that differences in values obtained in the present research and the study by Meigooni et al. in 2006 were less than 5% for both sources. These trivial differences may be due to variations in source materials, geometry definition and cross-section libraries in these studies.

The comparison of results of table 6, and those obtained by Meigooni et al. at different distances from the source showed a close agreement. For instance, the value of $g(r)_{w,solid\ water}^{w,w}$ at a 5 cm distance from the Pd-103 source was found to be 1.175, according to the fitted equation $0.95 + 0.045 \times (5cm)$ in this study. This value was close to the value obtained by Meigooni et al. (1.15), with about a 2% difference (14). The corresponding value for I-125 at a 5 cm distance was equal to 1.10 by the equation $0.965 + 0.027 \times (5cm)$, which was close to the value reported in the mentioned study (1.12), with less than a 2% difference (14).

5. Conclusion

The TG-43 parameters of low- and high-energy brachytherapy sources such as Pd-103, I-125 and Cs-137 were obtained in different phantoms. According to TG-43U1 recommendations by AAPM, the dosimetric characteristics of all brachytherapy sources should be obtained in liquid water phantoms. Experimentally, dose measurements in water are difficult; therefore, the measurements are performed in water-equivalent solid phantoms.

The attenuation properties of solid phantoms are different from water; therefore, the dose at different points in these phantoms is not exactly the same as water. In this study, Monte Carlo simulations of brachytherapy sources were performed in various phantoms, i.e., water, solid water, lucite, polyethylene, polystyrene, soft tissues and muscles. The results indicated that conversion factors are necessary for converting dose-to-water values in phantoms to dose-to-water values in water phantoms, especially for low-energy sources. Polynomial coefficients of conversion factors, used to quantitatively compare $g(r)$ values in different phantom materials and the radial dose

function in water, were presented for various phantom materials. By using these conversion factors, one can easily convert the measured dose to water in solid phantoms to the dose to water in water phantoms in order to be consistent with TG-43 recommendations.

Therefore, the experimental measurements in solid phantoms can be used for obtaining consensual data on radial dose function. In fact, the conversion factors presented in this study are quite useful in the estimation of dose in water. Finally, conversion factors were proposed for estimating dose to muscle and soft tissues from $D_{w,w}$, to be used in treatment planning systems.

The results of this study indicated that solid water phantom is a suitable water-equivalent phantom for obtaining the dosimetric parameters of low-energy photon-emitting brachytherapy sources. Other phantoms such as polystyrene, polyethylene and PMMA need larger conversion factors to become equivalent to water. In high-energy sources, we can use all the mentioned phantoms without any conversion factors.

References

1. Rivard MJ, Coursey BM, DeWerd LA, Hanson WF, Huq MS, Ibbott GS, et al. Update of AAPM Task Group No. 43 Report: A revised AAPM protocol for brachytherapy dose calculations. *Med Phys.* 2004 Mar;31(3):633-74.
2. Nath R, Anderson LL, Luxton G, Weaver KA, Williamson JF, Meigooni AS. Dosimetry of interstitial brachytherapy sources: recommendations of the AAPM Radiation Therapy Committee Task Group No. 43. *American Association of Physicists in Medicine. Med Phys.* 1995 Feb;22(2):209-34.
3. Perez-Calatayud J, Granero D, Ballester F, Puchades V, Casal E. Monte Carlo dosimetric characterization of the Cs-137 selectron/LDR source: Evaluation of applicator attenuation and superposition approximation effects. *Medical physics.* 2004;31(3):493-9.
4. Meigooni AS, Meli JA, Nath R. A comparison of solid phantoms with water for dosimetry of 125I brachytherapy sources. *Medical physics.* 1988;15(5):695-701.
5. Reniers B, Verhaegen F, Vynckier S. The radial dose function of low-energy brachytherapy seeds in different solid phantoms: comparison between calculations with the EGSnrc and MCNP4C Monte Carlo codes and measurements. *Physics in medicine and biology.* 2004;49(8):1569.
6. Patel NS, Chiu-Tsao S-T, Williamson JF, Fan P, Duckworth T, Shasha D, et al. Thermoluminescent dosimetry of the Symmetra125I model I25. S06 interstitial brachytherapy seed. *Medical physics.* 2001;28(8):1761-9.
7. Meli JA, Meigooni AS, Nath R. On the choice of phantom material for the dosimetry of 192Ir sources. *International Journal of Radiation Oncology* Biology* Physics.* 1988;14(3):587-94.
8. Williamson JF. Comparison of measured and calculated dose rates in water near I-125 and Ir-192 seeds. *Medical physics.* 1991;18(4):776-86.
9. Melhus CS, Rivard MJ. Approaches to calculating AAPM TG-43 brachytherapy dosimetry parameters for 137Cs, 125I, 192Ir, 103Pd, and 169Yb sources. *Medical physics.* 2006;33(6):1729-37.

10. Carlsson Tedgren Å, Alm Carlsson G. Influence of phantom material and dimensions on experimental Ir-192 dosimetry. *Medical physics*. 2009;36(6):2228-35.
11. Sina S, Faghihi R, Soleimani Meigooni A, Siavashpour Z, Mosleh-Shirazi MA. Developing a Treatment Planning Software Based on TG-43U1 Formalism for Cs-137 LDR Brachytherapy. *Iran Red Crescent Med J*. 2013 Aug;15(8):712-7.
12. Sina S, Faghihi R, Meigooni AS, Mehdizadeh S, Mosleh Shirazi MA, Zehtabian M. Impact of the vaginal applicator and dummy pellets on the dosimetry parameters of Cs-137 brachytherapy source. *J Appl Clin Med Phys*. 2011;12(3):3480.
13. Meigooni AS, Li Z, Mishra V, Williamson JF. A comparative study of dosimetric properties of Plastic Water and Solid Water in brachytherapy applications. *Med Phys*. 1994 Dec;21(12):1983-7.
14. Meigooni AS, Awan SB, Thompson NS, Dini SA. Updated Solid Water to water conversion factors for 125I and 103Pd brachytherapy sources. *Med Phys*. 2006 Nov;33(11):3988-92.
15. Meigooni AS, Hayes JL, Zhang H, Sowards K. Experimental and theoretical determination of dosimetric characteristics of IsoAid ADVANTAGE 125I brachytherapy source. *Medical physics*. 2002;29(9):2152-8.
16. Solberg TD, DeMarco JJ, Hugo G, Wallace RE. Dosimetric parameters of three new solid core I-125 brachytherapy sources. *Journal of Applied Clinical Medical Physics*. 2002;3(2):119-34.
17. Zehtabian M, Sina S, Faghihi R, Meigooni A. Perturbation of TG-43 parameters of the brachytherapy sources under insufficient scattering materials. *J Appl Clin Med Phys*. 14(3):4228.
18. Meigooni AS, Bharucha Z, Yoe-Sein M, Sowards K. Dosimetric characteristics of the bests double-wall 103Pd brachytherapy source. *Medical physics*. 2001;28(12):2568-75.
19. Peterson SW, Thomadsen B. Measurements of the dosimetric constants for a new 103Pd brachytherapy source. *Brachytherapy*. 2002;1(2):110-9.
20. Mosleh Shirazi MA, Faghihi R, Siavashpour Z, Nedaie HA, Mehdizadeh S, Sina S. Independent evaluation of an in-house brachytherapy treatment planning system using simulation, measurement and calculation methods. *J Appl Clin Med Phys*. 13(2):3687.
21. Briesmeister JF. MCNPTM-A general Monte Carlo N-particle transport code. Version 4C, LA-13709-M, Los Alamos National Laboratory. 2000.
22. Carlsson Tedgren A, Carlsson GA. Influence of phantom material and dimensions on experimental 192Ir dosimetry. *Med Phys*. 2009 Jun;36(6):2228-35.
23. Kirov AS, Williamson JF, Meigooni AS, Zhu Y. Measurement and calculation of heterogeneity correction factors for an Ir-192 high dose-rate brachytherapy source behind tungsten alloy and steel shields. *Med Phys*. 1996 Jun;23(6):911-9.
24. McConn Jr RJ, Gesh CJ, Pagh RT, Rucker RA, Williams Iii R. Compendium of Material Composition Data for Radiation Transport Modeling. PNNL-15870 Rev. 2011;1.
25. Luxton G. Comparison of radiation dosimetry in water and in solid water phantom materials for I-125 and Pd-103 brachytherapy sources:EGS4 Monte Carlo study. *Med Phys*. 1994;21(5):631-41.
26. Luxton G, Astrahan MA, Findley DO, Petrovich Z. Measurement of dose rate from exposure-calibrated 125I seeds. *Int J Radiat Oncol Biol Phys*. 1990 May;18(5):1199-207.